

## Quenching of the Quantum Hall Effect in Multilayered Epitaxial Graphene: The Role of Undoped Planes

Pierre Darancet,<sup>1</sup> Nicolas Wipf,<sup>1</sup> Claire Berger,<sup>1,2</sup> Walt A. de Heer,<sup>2</sup> and Didier Mayou<sup>1</sup>

<sup>1</sup>*Institut Néel, CNRS/UJF, 25 rue des Martyrs BP166, 38042 Grenoble Cedex 9, France*

<sup>2</sup>*School of Physics, Georgia Institute of Technology, Atlanta, Georgia 30332, USA*

(Received 8 November 2007; published 10 September 2008)

We propose a mechanism for the quenching of the Shubnikov–de Haas oscillations and the quantum Hall effect observed in epitaxial graphene. Experimental data show that the scattering time of the conduction electron is magnetic field dependent and of the order of the cyclotron orbit period, i.e., it can be much smaller than the zero field scattering time. Our scenario involves the extraordinary graphene  $n = 0$  Landau level of the uncharged layers which is pinned at the Fermi level. We find that the coupling between this  $n = 0$  Landau level and the conducting states of the doped plane leads to a scattering mechanism having the right magnitude to explain the experimental data.

DOI: [10.1103/PhysRevLett.101.116806](https://doi.org/10.1103/PhysRevLett.101.116806)

PACS numbers: 73.63.Bd, 73.43.-f, 81.05.Uw

Electrons in two-dimensional graphene obey an effective Dirac equation, in the continuum limit, and their properties are fundamentally different from those of electrons in standard semiconductors which obey the Schrödinger equation. A remarkable example is the quantum Hall effect which is quantized with integer plus half values [1,2] and has even been observed at room temperature [3]. Another major fact is the large electronic coherence [4,5], which is observed even at room temperature and gives hope to the possibility of producing devices with new properties. Graphene can be either exfoliated [1,2] or epitaxial [4–7]. Both methods produce graphene samples with spectacular electron coherence properties. Yet magnetotransport remains puzzling in epitaxial graphene. On one hand, at low magnetic field, the experimental results indicate electronic mean free paths of more than half a micron at 4 K [5,8]. On the other hand, Shubnikov–de Haas oscillations of the magnetoresistance are weak and the quantum Hall effect is not observed. Here we show, by analyzing the experimental data, that the results can be explained by a scattering time of the conduction electron which is magnetic field dependent, and reduced to the order of the cyclotron orbit period. We argue that the conducting states in a doped layer can couple to the zeroth Landau levels in an undoped layer, which is on top of the doped one. As a consequence, the conducting electrons of the doped layer are subjected to a scattering mechanism that increases with magnetic field because the number of states in the zeroth Landau level increases with magnetic field. At low magnetic field the scattering time  $\tau$  can be long but at stronger field  $\tau$  decreases in such a way that  $\omega\tau \approx 1$ , where  $\omega$  is the cyclotron frequency. This forbids the observation of strong Shubnikov–de Haas oscillations. We show also that in some limits the magnetoresistance increases linearly with the magnetic field. This has been observed recently in epitaxial graphene multilayers, and the magnitude of the linear magnetoresistance is in quantitative agreement with our model.

In this Letter, we present first the experimental results, and show that they can be explained by a linear dependence of the scattering rate with the magnetic field. Based on experiments we propose a simple model of electronic structure which we analyze. The magnetotransport properties of this model are in good agreement with the experimental observations.

*Summary of previous experimental results.*—Electronic properties of epitaxial graphene have been analyzed in great detail. They clearly point to the existence of an electron-doped plane at the SiC/graphene interface [9,10] carrying the main part of the current [5]. Since the screening length is of 1–2 interlayer spacing, only 2–3 planes are doped, and the other planes are quasineutral, as shown in infrared spectroscopy [11], and are thus comparatively poor conductors. The experimental evidence that one of the doped planes carries the main part of the current suggests that the other doped planes have a low conductivity due to the impurities' spatial distribution. The doped and quasineutral planes all have the characteristics of an isolated graphene plane, i.e., massless Dirac electrons [5,9–11]. This was initially surprising since the epitaxial graphene samples studied in [5,11] consist of several stacked graphene planes. Yet, as proven recently, these planes are rotationally stacked [12] and the relative rotation strongly diminishes the effective electronic coupling between the planes as compared to the case of *A-B* (Bernal) stacking [12–16].

*Analysis and interpretation of experimental results.*—The magnetotransport coefficients  $\rho_{xx}$  and  $\rho_{xy}$  for three samples of various widths (0.27, 5, and 1000  $\mu\text{m}$ ) are plotted in Fig. 1. Because the quantum corrections to the conductivity are small [8] a semiclassical one band model should be a fair approximation. The transverse magnetoresistance  $\rho_{xy}$  increases essentially linearly with the magnetic field  $B$  and is indeed consistent with a semiclassical model. Yet, the longitudinal magnetoresistance  $\rho_{xx}$  increases linearly with  $B$ .

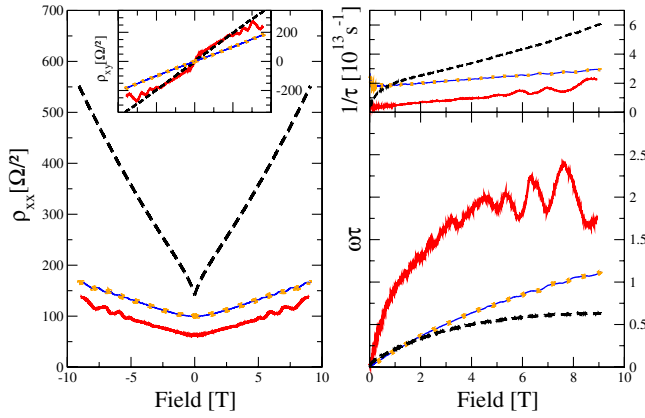


FIG. 1 (color online). Left: Experimental values of resistivity as a function of  $B$  for a  $100 \mu\text{m} \times 1000 \mu\text{m}$  (dashed line), a  $1 \mu\text{m} \times 5 \mu\text{m}$  (dash-dotted line), and a  $0.27 \mu\text{m} \times 6 \mu\text{m}$  (full line) sample. Main panel: Longitudinal magnetoresistance  $\rho_{xx}$ ; inset: transverse magnetoresistance  $\rho_{xy}$ . Right:  $\rho_{xy}/\rho_{xx}$  (which is equal to  $\omega\tau$  in the one band model) (bottom panel) and deduced scattering rate (top panel). Note that the longitudinal magnetoresistances  $\rho_{xx}$  have already been published in the case of the  $0.27 \mu\text{m} \times 6 \mu\text{m}$  [5] and the  $100 \mu\text{m} \times 1000 \mu\text{m}$  [8] samples.

From these experimental results, it is possible to plot the ratio  $\omega\tau$  and consequently to extract the scattering rate  $1/\tau$  (Fig. 1). This clearly indicates that the scattering rate linearly increases with the magnetic field. We note that there is also experimental evidence from optical measurements that the scattering rate increases with increasing magnetic field in these systems as it does in graphite [17]. Since  $\omega$  is given by  $\hbar\omega = \frac{eBV_F}{k_F}$  (where  $\hbar\omega$  corresponds to the level spacing between two Landau levels), and is linear with  $B$ , we can deduce from experiments

$$\frac{\hbar}{\tau(B)} \simeq \frac{\hbar}{\tau(B=0)} + \gamma\hbar\omega, \quad (1)$$

where  $\gamma$  is a positive constant. Note that  $1/\tau(B) > 1/\tau(B=0)$ , and  $\omega\tau < 1/\gamma$  (with  $\gamma$  equal to 0.4, 0.45, and 1.25 for the present  $1 \mu\text{m} \times 5 \mu\text{m}$ ,  $0.27 \mu\text{m} \times 6 \mu\text{m}$ , and  $100 \mu\text{m} \times 1000 \mu\text{m}$  samples). Moreover, we clearly see (Fig. 1) that  $\omega\tau$  is directly related to the system's ability to exhibit Shubnikov–de Haas oscillations: At low  $\omega\tau$ , the system does not exhibit such oscillations, while higher values are concomitant with the appearance of well-separated Landau level in the electronic structure. A scattering rate  $1/\tau$  linear with  $B$  can thus explain both the unusual magnetoresistance behavior and the quenching of Shubnikov–de Haas oscillations. If one assumes that the coupling between the different planes is negligible, it might seem quite difficult to explain a scattering rate that varies linearly with the magnetic field. Indeed, the conventional theory only predicts a quadratic correction to the magnetoresistance [18]. Yet, a scattering mechanism due to coupling between the doped and undoped planes will

depend on the magnetic field since the electronic structure of the undoped planes depends on the magnetic field. Even in weak magnetic fields the Fermi level in the nearly neutral planes will be in the low index Landau levels and it will be in the zeroth Landau level as soon as  $B > B_C = \hbar n_d/2e$ , where  $n_d$  is the electron density. Infrared Landau spectroscopy for the nearly undoped planes indicates  $n_d$  is less than  $10^{10} \text{ cm}^{-2}$ , i.e.,  $B_C \ll 1 \text{ T}$  [11]. We will see that this scattering mechanism implies an increasing scattering rate with an order of magnitude of  $\Delta[\hbar/\tau(B)] \simeq \hbar\omega$ , with  $\gamma$  close to 1, compatible with the experiments.

*Model of electronic structure.*—We consider that the perfect rotationally stacked planes are essentially decoupled since the coupling between different states close to the Dirac point is of the order of 1 meV (compared to 0.2–0.3 eV for A-B stacking) [12]. It is important to note that the hopping matrix elements between neighboring orbitals of the two rotated planes are of the order of 0.2–0.3 eV, and that the effective electronic decoupling is due to an averaging specific to the perfect structure. This averaging is destroyed by disorder, and consequently the defects in one plane will introduce a scattering in that plane and a coupling with electronic states in the other plane. Defects that spread on both planes also introduce in-plane scattering and interplane coupling. Here we consider a model with one doped plane and one plane which is essentially neutral, for which the zeroth Landau level is half filled at all values of the magnetic field. The two planes are decoupled in the absence of disorder but are coupled by disorder. In the following plane 1 is the doped plane and plane 2 the undoped one.

We consider also that the electronic states in plane 1 are coupled essentially to the zeroth order Landau level of plane 2 only. Indeed, we note that for  $B = 1 \text{ T}$  the index of the Landau levels of the doped plane is  $n \simeq 30\text{--}40$  and there are about  $2N_L \simeq 15$  Landau levels of the doped plane which are closer to the zeroth Landau level than to the other Landau levels of plane 2. In the following we shall treat  $N_L$  as a large number.

The model for the Green functions of the uncoupled and perfect planes 1 and 2 are  $G_{1,0}(z)$  and  $G_{2,0}(z)$ :

$$G_{1,0}(z) = \sum_{n=-N_L}^{n=N_L} \frac{N(B)}{z - n\hbar\omega}, \quad G_{2,0}(z) = \frac{RN(B)}{z - E_{L0}}, \quad (2)$$

with  $\hbar\omega = \frac{eBV_F}{k_F}$  and  $\frac{N(B)}{\hbar\omega} = n_0 = \frac{2k_F}{\pi\hbar v_F}$ .  $k_F$  is the Fermi wave vector of the doped plane and  $n_0$  its density of states at the Fermi energy, without magnetic field. In this model we assume that the Landau levels of plane 1 are equally spaced by  $\hbar\omega$  where  $\omega$  is the cyclotron frequency (which is valid as long as their index is high).  $E_{L0}$  is the energy of the zeroth Landau level ( $E_{L0} \ll N_L\hbar\omega$  varies with  $B$  so that the zeroth Landau level stays half filled), and  $R$  is the ratio between the number of states in the zeroth Landau level of plane 2 and in a Landau level of plane 1.  $R$  is equal to 1 if

the two planes are equivalent (apart from the doping). We can also simulate the case where the doped plane is coupled to two undoped planes by taking  $R = 2$ . The degeneracy of a zeroth Landau level of a bilayer in  $A$ - $B$  stacking is also  $R = 2$  [19]. Thus different configurations can lead to different values of  $R$ , and this parameter is adjustable in the following.

In order to treat the effect of in-plane scattering by disorder and intraplane coupling by disorder we use a standard self-consistent Born approximation (SCBA). Despite its limitations, SCBA constitutes the “standard” simplest approximation for the description of the coupling potential effect on the electronic structure. Since we are interested in the description of the electronic structure close to the Fermi energy, this approximation will provide us with a self-consistent Fermi golden rule picture. We introduce the Green function  $G_P(z)$  and the self-energies  $\Sigma_P(z)$  of plane “ $P$ ” ( $P = 1$  or  $P = 2$ ). The density of states per unit surface in plane  $P$  is given by  $n_P(E) = -(1/\pi) \text{Im}[G_P(z = E + i\epsilon)]$ , where  $\epsilon$  is an infinitely small positive real number. One gets:

$$G_P(z) = G_{P,0}[z - \Sigma_P(z)] \quad (3)$$

$$\Sigma_P(z) = |V|^2 G_{P'}(z) - i \frac{\hbar}{2\tau_{P,P}}. \quad (4)$$

$P'$  is the plane coupled to plane  $P$  ( $P' = 1$  if  $P = 2$  and vice versa).  $V^2$  is an average value of the square coupling between states in plane 1 and in plane 2. This coupling strength between the states in planes 1 and 2 at the energies  $E_1$  and  $E_2$  is considered to be independent of  $E_1$  and  $E_2$ , due to the local nature of the interlayer interaction. In accordance with that, we assume that the change in eigenstates induced by the magnetic field does not affect the coupling strength. The terms  $\hbar/2\tau_{P,P}$  represent the effect of in-plane scattering for each plane  $P$  ( $\tau_{P,P}$  is the in-plane scattering time).

In Eqs. (2)–(4) the two important parameters for the effect of the interplane coupling are  $R$  and  $V$ . We analyze below the regimes of large and small  $R$  or  $V$ . We show that in the large  $V$  limit the experimental magnetic field dependence of the scattering rate (see Fig. 1) is explained with a reasonable value of the parameter  $R$ . We emphasize that the physics described below presents some analogies with the coupling between localized  $d$  orbitals with extended  $sp$  states [20].

*Large and small  $R$  regimes.*—In this part, we focus on the case  $z = E_{L0} + i\epsilon$ . Since the zeroth Landau level is half filled,  $E_{L0}$  is always close to the Fermi level. Let us assume that  $G_1(z = E_{L0} + i\epsilon) \simeq -i\pi n_0$  and thus  $n_1(E_{L0}) \simeq n_0$  (we show below that this corresponds to the large  $R$  limit). After (2)–(4), this occurs for  $|\text{Im}\Sigma_1(E_{L0} + i\epsilon)|/\hbar\omega \gg 1$ . In this limit, the real parts  $\text{Re}G_2(E_{L0} + i\epsilon)$ ,  $\text{Re}G_1(E_{L0} + i\epsilon)$ ,  $\text{Re}\Sigma_2(E_{L0} + i\epsilon)$ ,  $\text{Re}\Sigma_1(E_{L0} + i\epsilon)$  are all negligible. Using the correspondence  $\hbar/\tau = 2 \text{Im}\Sigma$ , where

$\tau$  is an electron lifetime, one may write the SCBA equations in a form similar to the Fermi golden rule, i.e.,  $\frac{\hbar}{\tau_P} = \frac{\hbar}{\tau_{P,P}} + 2\pi V^2 n_{P'}$  with  $n_1 \simeq n_0$  and  $n_2 = RN(B) \frac{2\tau_2}{\pi\hbar}$  the densities of states at  $z = E_{L0} + i\epsilon$ , and then

$$\frac{\hbar}{\tau_1} \simeq \frac{\hbar}{\tau_{1,1}} + \frac{2R}{\pi} \frac{\hbar\omega}{1 + \alpha}, \quad (5)$$

with  $\alpha = \frac{\hbar/\tau_{2,2}}{2\pi V^2 n_0}$ . Here  $\hbar/\tau_{2,2}$  and  $2\pi V^2 n_0$  are, respectively, the width of the zeroth Landau level due to disorder in plane 2 and to coupling with plane 1 in the limit where its density is  $n_0$ . One sees that if disorder in plane 2 (term  $\hbar/\tau_{2,2}$ ) increases then the scattering rate  $\hbar/\tau_1$  decreases. Indeed the scattering by plane 2 is favored by a strong density of states in plane 2, whereas the term  $\hbar/\tau_{2,2}$  tends to decrease this density. If  $\alpha \gg 1$ , the coupling between planes 1 and 2 has essentially no effect (i.e.,  $\omega\tau_1 \simeq \omega\tau_{1,1}$ ), but in the opposite limit  $\alpha \ll 1$  the scattering rate for electrons in plane 1 increases linearly with the magnetic field and  $\omega\tau_1 \leq \pi/2R$ .

We show now that one gets the regime  $G_1(z = E_{L0} + i\epsilon) \simeq -i\pi n_0$  at sufficiently large values of  $R$ . For simplicity we consider the limit  $\hbar/\tau_{2,2} = \hbar/\tau_{1,1} = 0$ , but let us just note that  $\hbar/\tau_{1,1}$  and  $\hbar/\tau_{2,2}$  have opposite effects, since  $\hbar/\tau_{1,1}$  favors the large  $R$  regime while  $\hbar/\tau_{2,2}$  favors a small  $R$  regime. The SCBA equations can be written with dimensionless quantities  $F_P = \tilde{F}_P(\frac{z}{\hbar\omega}, \frac{E_{L0}}{\hbar\omega}, \frac{2\pi V^2 n_0}{\hbar\omega}, R)$ , where  $F_P = \frac{G_P(z)}{n_0}$  or  $F_P = \frac{\Sigma_P(z)}{\hbar\omega}$ . At  $z = E_{L0} + i\epsilon$  one get for  $G_1(z)$ , after (2)–(4),  $G_1(z) = G_{1,0}[z - R \frac{N(B)}{G_1(z)}]$ . This equation is independent of the coupling parameter  $V$ , and in that case  $n_1/n_0$  and  $2 \text{Im}\Sigma_1/\hbar\omega = 1/\omega\tau_1$  are functions only of  $E_{L0}/\hbar\omega$  and  $R$ .

We consider  $E_{L0}/\hbar\omega = 0$  and  $E_{L0}/\hbar\omega = 1/2$  for which by symmetry  $E_{L0} = E_F$  and the real parts of the self-energies and Green’s functions are zero. The result is shown in Fig. 2. For large  $R$ , typically  $R \gtrsim 1.5$ – $2$ , one has  $n_1(E_F)/n_0 \simeq 1$ , which is the criterion for the strong scattering regime. In that case one recovers the strong scattering limit  $\hbar/\tau_1 \simeq 2R/\pi\hbar\omega$  that is  $\omega\tau_1 = \pi/2R$ . Note also that in the large  $R$  regime the results are essentially independent of  $E_{L0}/\hbar\omega$ . At  $R = 1$  (i.e., not in the large  $R$  regime) and for  $E_{L0}/\hbar\omega = 0$  the density of states  $n_1(E_F)$  diverges. Indeed, as soon as  $R < 1$  there are less

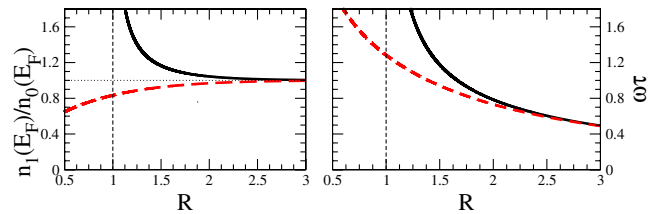


FIG. 2 (color online). Left: Value of  $n_1(E_F)/n_0$  as a function of  $R$  for  $E_{L0}/\hbar\omega = 0$  (full line) and for  $E_{L0}/\hbar\omega = 1/2$  (dashed line). Right: Same for the ratio  $\omega\tau_1$ .

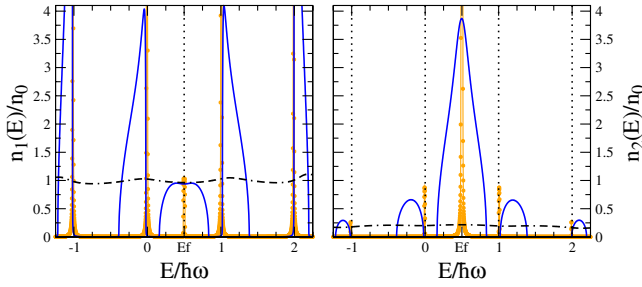


FIG. 3 (color online). Left: Dimensionless density of states in plane 1 [ $n_1(E)/n_0$ ] as a function of energy for different coupling  $V^2 n_0/\hbar\omega = 1$  (dash-dotted line);  $6 \times 10^{-2}$  (full line);  $1 \times 10^{-3}$  (dotted line) and  $R = 2$ ,  $E_{L0}/\hbar\omega = 1/2$ . Right: Same for the dimensionless density of states [ $n_2(E)/n_0$ ] in plane 2.

states in the zeroth Landau level of plane 2 than in Landau levels of plane 1. This means that there exist uncoupled states of the Landau level of plane 1 and thus an infinite density  $n_1(E_F)$  as soon as  $R < 1$ .

*Large and small  $V$  regimes.*—We define the large and small  $V$  regimes, respectively, by  $2\pi V^2 n_0/\hbar\omega \gg 1$  and  $2\pi V^2 n_0/\hbar\omega \ll 1$ . After the dimensional analysis the width  $W$  of the zeroth Landau level of plane 2 and thus the energy range on which the electronic structure is modified by the coupling satisfies  $W/\hbar\omega = \tilde{W}(E_{L0}/\hbar\omega, V^2 n_0/\hbar\omega, R)$ .

In the large  $V$  regime, as long as  $|z - E_{L0}|/\hbar\omega \leq 2\pi V^2 n_0/\hbar\omega$  the term  $|z - E_{L0}| \ll |V^2 G_1(z)|$  and one recovers  $G_1(z) = G_{1,0}[z - R \frac{N(B)}{G_1(z)}]$ . The dimensionless  $G_1(z)/n_0$  and  $\Sigma_1(z)/\hbar\omega$  depend on  $z/\hbar\omega$  and  $R$  but not on  $E_{L0}/\hbar\omega$  and  $2\pi V^2 n_0/\hbar\omega$ . Note that the periodicity  $\hbar\omega$  of  $G_{1,0}(z = E + i\epsilon)$  (2) implies the same periodicity for  $G_1(z = E + i\epsilon)$  and  $n_1(E)$  in this limit. For the density of states in plane 2 one has after (2)–(4)  $n_2(E)/n_0 = (R/\pi^2)(\hbar\omega/V^2 n_0)[n_0/n_1(E)]$ . Thus  $n_2(E)/n_0$  presents the same periodicity (within the range  $W$ ) and is very small. The spectral weight  $RN(B)$  of the zeroth Landau level spreads on a width  $W$ , and thus since  $n_2(E)/n_0 \simeq (R/\pi^2)(\hbar\omega/V^2 n_0)$  one has  $W/\hbar\omega \simeq \pi^2 V^2 n_0/\hbar\omega$ . Finally, in the small  $V$  regime  $2\pi V^2 n_0/\hbar\omega \ll 1$  the width  $W/\hbar\omega \ll 1$  and the Landau levels of plane 1 and 2 are only slightly hybridized (see Fig. 3).

*Magnetotransport.*—When the density of states is uniform on an energy scale  $W \gg \hbar\omega$ , which is the case in the large  $R$  and  $V$  regime (see Fig. 3), we can apply the semiclassical theory of transport. The scattering time  $\tau_1$  is given by  $\hbar/\tau_1 = \hbar/\tau_{1,1} + 2\hbar\omega R/[\pi(1 + \alpha)]$ , where  $\hbar/\tau_{1,1}$  is the in-plane scattering rate. As long as  $\alpha$  is not too large we expect the term  $2\hbar\omega R/[\pi(1 + \alpha)]$  to be of order  $\hbar\omega$  and the model is consistent with the experimental results presented above [see Fig. 1 and Eq. (1)].

Shubnikov–de Haas oscillations can occur when the field dependent scattering studied here is destroyed, that is, for  $\alpha \gg 1$ . This can be due, for example, to disorder in plane 2 or even to a confinement effect as in a ribbon of finite width [21], as in Fig. 1. Shubnikov–de Haas oscillations can thus be enhanced by disorder or by confinement effects. This spectacular effect is clearly observed in experiments [4].

To conclude, we have shown that the quenching of the Shubnikov–de Haas oscillations and of the quantum Hall effect on epitaxial graphene is consistent with a scattering time that is magnetic field dependent and is reduced to the order of the cyclotron period. This can be explained by a mechanism where the conducting electrons of the doped plane are scattered due to their coupling with the zeroth Landau level of the undoped planes.

We thank X. Wu, L. Magaud, V. Olevano, G. Trambly de Laissardière, and F. Varchon for many stimulating exchanges. One of us (D.M.) also thanks Pascale Lefebvre. We acknowledge a travel grant from CNRS-DREI, and NSF funding under Grant No. 4106A68 and the W.M. Keck Foundation.

- 
- [1] K. S. Novoselov *et al.*, Nature (London) **438**, 197 (2005).
  - [2] Y. Zhang *et al.*, Nature (London) **438**, 201 (2005).
  - [3] K. S. Novoselov *et al.*, Science **315**, 1379 (2007).
  - [4] W. A. de Heer *et al.*, Solid State Commun. **143**, 92 (2007).
  - [5] C. Berger *et al.*, Science **312**, 1191 (2006).
  - [6] C. Berger *et al.*, J. Phys. Chem. B **108**, 19912 (2004).
  - [7] J. Hass *et al.*, Appl. Phys. Lett. **89**, 143106 (2006).
  - [8] X. Wu *et al.*, Phys. Rev. Lett. **98**, 136801 (2007).
  - [9] E. Rollings *et al.*, J. Phys. Chem. Solids **67**, 2172 (2006).
  - [10] T. Ohta *et al.*, Science **313**, 951 (2006).
  - [11] M. L. Sadowski *et al.*, Phys. Rev. Lett. **97**, 266405 (2006).
  - [12] J. Hass *et al.*, Phys. Rev. Lett. **100**, 125504 (2008).
  - [13] J. M. B. Lopes dos Santos *et al.*, Phys. Rev. Lett. **99**, 256802 (2007).
  - [14] S. Latil *et al.*, Phys. Rev. Lett. **97**, 036803 (2006).
  - [15] S. Latil *et al.*, Phys. Rev. B **76**, 201402 (2007).
  - [16] F. Ducastelle and P. Quémerais, Phys. Rev. Lett. **78**, 102 (1997).
  - [17] Z. Q. Li *et al.*, Phys. Rev. B **74**, 195404 (2006); G. Martinez (private communication).
  - [18] A. A. Abrikosov, *Fundamentals of the Theory of Metals* (North-Holland, Amsterdam, 1988).
  - [19] E. McCann and V. I. Fal’ko, Phys. Rev. Lett. **96**, 086805 (2006).
  - [20] C. Berger *et al.*, Ann. Chim. (Paris) **18**, 485 (1993); E. Belin and D. Mayou, Phys. Scr. **T49a**, 356 (1993); G. Trambly de Laissardière *et al.*, Prog. Mater. Sci. **50**, 679 (2005).
  - [21] N. M. R. Peres *et al.*, Phys. Rev. B **73**, 241403(R) (2006).